

Fabrication and Characterization of an Amperometric Glucose Sensor on a Flexible Polyimide Substrate

Xiaosong Du,¹ Christopher J. Durgan,¹ David J. Matthews,² Joshua R. Motley,¹ Xuebin Tan,²
Kovit Pholsena,¹ Líney Árnadóttir,¹ Jessica R. Castle³, Peter G. Jacobs^{3,4}, Robert S. Cargill³, W.
Kenneth Ward^{3,a}, John F. Conley Jr.^{2,a}, Gregory S. Herman^{1,a}

¹School of Chemical, Biological, and Environmental Engineering,

²School of Electrical Engineering and Computer Science,

Oregon State University, Corvallis, Oregon, 97331, USA

³Pacific Diabetes Technologies, Portland, Oregon, 97201, USA

⁴Oregon Health & Science University, Portland, Oregon, 97239, USA

^aAuthors to whom correspondence should be addressed. Electronic mail: kward@pacificdt.com,
john.conley@oregonstate.edu, and greg.herman@oregonstate.edu.

KEYWORDS: micro-contact printing, electrohydrodynamic printing, continuous glucose monitoring sensor, type 1 diabetes.

ABSTRACT

This study details the use of printing and other additive processes to fabricate a novel amperometric glucose sensor. The sensor was fabricated using a Au coated 12.7 μm polyimide film as a starting material, where micro-contact printing, electrochemical plating and chloridization, electrohydrodynamic jet (e-jet) printing, and spin coating were used to pattern, deposit, print, and coat functional materials, respectively. We have found that e-jet printing was effective for the deposition and patterning of glucose oxidase inks between ~ 5 to 1000 μm in width, and we have demonstrated that the enzyme was still active after printing. The thickness of the permselective layer was optimized to obtain a linear response to glucose concentration up to 32 mM. For these sensors no response to acetaminophen, a common interfering compound, was observed.

Advances in accurate sensing of blood glucose concentrations have contributed to improved control of blood sugar levels for patients with type 1 diabetes. Type 1 diabetes is a pancreatic and endocrine disease in which blood glucose is poorly controlled because the patient's beta cells cannot generate sufficient insulin. Long-term exposure to elevated glucose levels can lead to complications such as retinopathy, neuropathy, nephropathy, and cardiac disease. There is no known cure for type 1 diabetes and it has traditionally been controlled by the use of frequent glucose measurement with a blood glucose meter and insulin injections in order to maintain blood glucose levels within an acceptable range. The recent development of continuous glucose sensors now allows real-time monitoring of blood sugar levels. Continuous subcutaneous insulin pumps can continuously deliver basal and bolus doses of insulin to assist in maintaining glycemic control.^{1,2}

A glucose sensor is a critical component of an artificial pancreas and research in this area has been extensive. An artificial pancreas integrates continuous glucose sensing with automated delivery of the hormones including insulin and glucagon to appropriately control glucose levels.³⁻⁶ The concept of a closed loop artificial pancreas has been around for many years, beginning with the work of Albisser et al..^{7,8} The number of research studies on artificial pancreas controllers has increased in recent years including those using model predictive controllers⁹⁻¹¹ and those using proportional integrative derivative (PID) or PID-like controllers.¹²⁻¹⁶

A sensor within an artificial pancreas needs to measure glucose concentrations over a wide range of concentrations typical found in patients with diabetes, i.e. 0-30 mM, and it needs to be accurate to minimize the risk of over/under delivery of insulin and glucagon. Other desirable characteristics of an artificial pancreas sensor are long working lifetime to minimize the inconvenience of replacing the device, and low cost to facilitate widespread usage.

Amperometric glucose sensors are specified to work for 7 days, and typically have a mean absolute relative difference (MARD, percent error) in the 12-18% range. Castle et al found that redundancy of sensing elements can somewhat reduce the MARD and can markedly reduce the frequency of very large egregious errors.¹⁷

Continuous glucose sensors have been made using a wide variety of substrates and electrode materials. Harrison et al.¹⁸ fabricated a glucose sensor based on a platinum wire, which was dip-coated with an active enzyme layer. Yu et al.¹⁹ designed a coiled platinum wire with an integrated Ag/AgCl reference electrode wire, which was successfully tested in rats for a period of up to 56 days. Endo et al.²⁰ developed another sensor with integrated Ag/AgCl reference electrode and a platinum wire which provided continuous glucose monitoring in anesthetized animals. Other glucose sensor devices have been fabricated on flexible polymer substrates. Kudo et al.²¹ constructed a sensor on a polydimethylsiloxane (PDMS) substrate, with platinum working electrode and Ag/AgCl counter/reference electrode. Sensors with the same design were also fixed to PDMS contact lenses and successfully tested in rabbits.²² Li et al.²³ used a polyimide substrate to fabricate a spirally rolled flow-through catheter for implantation in blood vessels. The sensor featured gold working and counter electrodes with a Ag/AgCl reference electrode.

In this paper, we demonstrate that printing and additive processes can be used to fabricate amperometric glucose sensors using a metallized thin, flexible polyimide substrate. High-resolution electrohydrodynamic (e-jet) printing was used to pattern functional glucose oxidase (GOx) enzyme inks on plated platinum working electrodes. Amperometric measurements performed with the working electrode biased 0.600 V, with respect to the Ag/AgCl reference electrode, indicates that the enzyme is still active after printing. The thickness of a permselective layer was optimized to limit the glucose diffusion rate to the GOx layer compared to oxygen

diffusion, which provides a linear response to glucose concentration. Our results illustrate that low cost manufacturing approaches can be used to fabricate amperometric glucose sensors, and can potentially be applied to other enzymatic sensing approaches.

Experimental

Materials

Bovine serum albumin (BSA), 1H,1H,2H,2H-perfluorodecanethiol, ferric nitrate, acetaminophen and octadecanethiol were purchased from Sigma Aldrich. Thiourea and glucose was obtained from Alfa Aesar. Glutaraldehyde was acquired from Electron Microscopy Sciences. Glucose oxidase and FeCl_3 were obtained from Amresco. NaCl , KCl , NaH_2PO_4 , Na_2HPO_4 were acquired from Macron. The e-jet printing needle (glass micropipette) was purchased from World Precision Instruments. Perfluorosulfonic acid (PFSA) in 1-propanol and water was purchased from Ion Source. The photoresist SU-8 was acquired from Microchem. Sylgard 184 PDMS was obtained from Dow Corning. The Pt and Ag plating solution were purchased from Technic. Au (150 nm thick) on 12.7 μm polyimide (PI) film was acquired from Sheldahl. Milli-Q water was used in all sample preparation.

Amperometric sensor electrode fabrication

Au was patterned on a Au/polyimide substrate by micro-contact printing technique as has been described previously.²⁴⁻²⁶ In brief, a PDMS stamp was fabricated from a SU-8 master that was patterned on a silicon substrate using photolithography. A self-assembled monolayer (SAM), octadecanethiol, was formed on the PDMS stamp by immersion in 2 mM octadecanethiol (ethanol as solvent) for 5 min. The SAM was transferred from the PDMS stamp to the Au on the

PI film after ~ 15 s contact time. After the SAM transfer the unprotected Au was etched at a rate of 10 nm/min in 20 mM Fe(NO₃)₃ and 30 mM thiourea solution at pH ~ 2.²⁷ The octadecanethiol SAM was removed from the Au surface by UV-Ozone treatment followed by an ethanol rinse. The surface was thoroughly cleaned by oxygen plasma (PE-100, Plasma Etch, Inc.).

Selective electroplating was performed by making electrical connection to the working or reference electrode contact pads. ~12 nm Pt was electroplated on the working electrodes at a plating bath temperature of 65 °C and a current density ~ 54 A/m² for 40s, ~200 nm Ag was electroplated on counter/reference electrode at a plating bath temperature of 30 °C and a current density ~ 107 A/m² for 25s. Chloridization of the Ag was performed by reacting the Ag electrode with a 50 mM FeCl₃ solution for 2 min.²⁸ The chloridization was performed soon after electroplating to minimize the formation of silver oxide and silver sulfide. A uniform layer of sub-micron AgCl particles can be observed after chloridization and electroplated Ag showed homogeneous coverage on Au/PI film.

Electrohydrodynamic printing

A custom-built e-jet printer was used to deposit and pattern GOx ink onto the Pt working electrodes. The e-jet printer features a high-voltage amplifier (Trek 677B), which applies a voltage between the printing needle and the substrate. The substrate is placed on a carrier that has computer controlled x and y-axis linear stepper motorized stages (Parker MX80L T03MP), and a two-axis tilting stage (Edmund Optics 70mm metric Micrometer Tilt Stage) to level the substrate. The printing needle can be moved up and down using a computer controlled z-axis linear stepper motor (Parker MX80ST 02MSJ). The printing process was observed through a microscope camera (Edmund Optics Infinity2) illuminated with fiber optic lamps. Custom control software was written in LabView. The printing needle was coated with a thin sputtered film of 60/40

Au/Pd alloy to provide electrical conductivity, using a Cressington Sputter Coater 108auto. Needles with an inner diameter tip of 5 and 30 μm were used for these experiments. Prior to printing, the needle tip was dipped in liquid 1H,1H,2H,2H-perfluorodecanethiol for one minute, which forms a hydrophobic SAM on the outer metal surface of the needle. This monolayer prevents excessive wetting of the needle by the GOx ink. Air pressure was controlled by a pressure transducer (ControlAir 500-AF) that was connected to a syringe and forced the ink to the tip of the needle. Normal operating pressures were between 0.5 and 3 psi. The needle bias was set using a National Instruments controller (SCB-80) to the voltage amplifier, which was connected to the printing needle. Printing was achieved by pulsing the voltage in a square wave, where the frequency and amplitude of the wave were controlled by the software. To print in the controlled cone-jet mode, the lower voltage of the pulse was sufficient to hold the fluid meniscus in a Taylor cone whereas the higher voltage of the pulse caused fluid to eject from the tip of the cone.²⁹⁻³¹ To print specific patterns, the e-jet printing software reads a text file which contains commands to move the x- and y- stages, and to turn the voltage on or off. Modifying the stage velocity and voltage pulsing frequency allows the control of droplet size and spacing between droplets. Prior to printing the substrate was treated with UV/ozone for 15 min to ensure good surface wetting. The printed patterns were characterized using atomic force microscopy (AFM, Veeco Innova), optical microscopy (Zeiss Axiotron), and ZeScope (Zemetrics).

Glucose oxidase ink

An aqueous functional ink containing GOx and BSA was used for e-jet printing enzyme films. The dissolved GOx was stabilized with the addition of 5% v/v of glycerol to the aqueous base. The glycerol helps to keep the enzyme from crystallizing prematurely, and lowers surface tension of the ink, which aids in printing. It was determined that a mixture of 18mg GOx and 2

mg BSA per mL of water gave good mechanical stability of the enzyme layer, and maximized sensitivity to glucose. The total concentration of 20 mg/mL gave a thick enzyme layer once cross-linked, while still having properties that allowed consistent printing. In order to crosslink the GOx film onto the sensor device, the GOx and BSA were pre-mixed with 0.4 mg/mL glutaraldehyde just prior to printing on the Pt sensor surface.

Permselective membrane

PFSA in 1-propanol and water containing between 1% and 30% by weight of polymer were used to fabricate thin polymer films onto surfaces by spin-coating (Laurell WS-400BZ-6NPP/LITE), using rotation speeds of 1000-3000 RPM for 60-90 seconds. Polymer film thicknesses were measured by profilometry.

Electrochemical glucose sensing

Characterization of glucose sensor devices was performed by placing the sensor in an electrochemical cell containing 150 mM phosphate buffered saline (PBS) solution composed of NaCl, KCl, NaH₂PO₄, and Na₂HPO₄. The Pt working electrodes were polarized at +600 mV relative to the Ag/AgCl reference electrode. The electrochemical cell solution was purged with Ar during experiments, in order to stir the solution and reduce oxygen levels in the solution to that of mammalian interstitial fluid (45 torr or 0.08 mM).³² Amperometric measurements were obtained with a BioLogic SP-200 Potentiostat. Oxygen concentrations were measured with a NeuLog NEU-205 oxygen sensor. The chronoamperometric current between the working and reference/counter electrodes was monitored over time, while the concentration of glucose in the electrochemical cell was intermittently increased by pipetting in a concentrated glucose solution.

The glucose concentration was varied between 0-32 mM, which corresponds to the relevant clinical blood glucose levels of diabetic patients.

Results and Discussions

Sensor design

In Figure 1 a and b we show a cross sectional schematic of the sensor with each of the layers labeled (not to scale), and the operational principle, respectively. The three key factors that allow accurate glucose sensing are formation of platinum electrodes with well-defined areas and good catalytic activity, deposition of glucose oxidase layers with uniform thickness, and use of permselective layers with good control over the effective diffusion rates of glucose and oxygen. Each of these processes will be discussed below.

In Figure 2 a we show a Au film on PI substrates that was patterned using microcontact printing and etching, and the patterns did not have any resolution loss or visible defects. The Au microelectrodes yield exceeded 90% for a batch of devices as determined by optical microscopy and two-point electrical. Patterned photoresist was used to define the region where the metals were electroplated on Au electrodes. Electroplating of either Pt or Ag layers was conducted by applying a potential to achieve the desired current density, while the substrate was in the appropriate plating solution. The film thickness of plated Ag (200 nm) and Pt (12 nm) was determined by profilometry, and the plated Ag counter/reference electrode and Pt working electrodes are shown in Figure 2 b. Each working electrode has a planar surface area of approximately 0.32 mm^2 , whereas the total reference electrode area was approximately 4.74 mm^2 . A $2 \text{ }\mu\text{m}$ thick SU-8 layer was used as a passivation layer on the sensor and to provide wells for the working or counter/reference electrodes.

Electrohydrodynamic printing

Printing parameters on the e-jet printer (voltage, pulse frequency, stage velocity, pressure, and working distance) were adjusted to give repeatable patterning. Initially, the e-jet process deposited individual droplets. As the process was optimized, it became possible to print lines, and finally continuous films of GOx onto the flexible Pt/Au/PI substrates. Most printing was accomplished with a constant voltage of 600-800V, which was pulsed to 800 V with a frequency of 10-30 Hz. The distance between the printing needle and the substrate was typically 30-60 microns. The printed GOx patterns were characterized by optical microscopy and AFM to help optimize the printing parameters for uniform coverage of the electrode surfaces. To improve wetting of the GOx ink we performed a UV/ozone treatment of the Pt/Au/PI substrates prior to printing. E-jet printing allowed us to demonstrate printing of very small GOx features (droplets ~ 5 μm in diameter) which are shown in Figure 3. To optimize the parameters of e-jet printed GOx inks, different drop spacings were obtained by adjusting the stage velocity (v) and voltage square wave pulse frequency (f). Using a stage velocity of 1200 $\mu\text{m/s}$ and a frequency of 10 Hz (Figure 4 a), we found that the ratio of drop generation and the voltage frequency was ~ 1 . This ratio can be obtained up to $f = 20$ Hz (Figure 4 b), however above $f = 30$ Hz the printed drops (Figure 4 c) showed irregular size and/or spacing. This may be due to Taylor cone distortion with poor recovery at higher frequencies resulting in a reduction in the ratio of drop generation and the voltage frequency below 1.²⁹ Therefore, the optimized pulse frequency to print our GOx ink was determined to be 20 Hz, which allowed us to generate the most uniform drop patterns for high-speed printing. The stage velocity was also optimized to go from isolated droplets to continuous lines of GOx ink, by slightly overlapping each droplet with its previous neighbor. At a velocity of 1200 $\mu\text{m/s}$ and frequency of 20 Hz (Figure 4 d&g), multiple small droplets can be distinguished,

which results from multiple jetting processes during a single voltage pulse. When the velocity was slowed to 700 $\mu\text{m/s}$, the same frequency also gave multiple jets (Figure 4 e&h), however the individual droplets collected into larger elongated droplets. An even slower stage velocity of 500 $\mu\text{m/s}$ produced a smooth, continuous line with no evidence of individual droplets (Figure 4 f&i). The line width was determined to be approximately 30 μm wide for these printing conditions. Once fully connected lines were achieved, a pattern with line spacing of 30 μm was employed to create a fully covered film of GOx on Pt working electrodes as shown in Figure 5. It took approximately 1 min to print two layers on a single working electrode corresponding to a total printing time of 6 min for the entire device.

Electrochemical test

Spin-coating was used to provide a uniform film thickness for the PSM, and allowed us to evaluate the effect of PSM film thicknesses on sensor performance.^{33,34} It has been suggested that exposing the cross-linked GOx layer to concentrated acidic polymer solution may denature some of the enzyme.¹⁸ Therefore, a thin “base coat” of 1% PFSA, about 60 nm thick, was applied before subsequent applications of thicker membranes. Chronoamperometric data was obtained after application of the PSM on the flexible glucose sensors. Experimental data is shown in Figure 6 a where we monitored the amperometric current for three different PSM thicknesses. The current increases in a stepwise fashion as the glucose concentration is increased. The increase in amperometric current versus glucose concentration is shown in Figure 6 b. In the upper portion of Figures 6 a and b we show data from a two-coat membrane, with a total PFSA thickness of 300 nm. A highly nonlinear current response to glucose concentration was obtained, which suggests that the film does not effectively limit diffusion of glucose to the enzyme layer, and that the low oxygen concentrations limit the enzymatic reaction rate of H_2O_2 production. We

also found that using a 3 μm PFSA membrane significantly reduced the amperometric current (compared to the 300 nm PFSA membrane), but did not significantly extend the linear working range of the glucose sensor. This sensor only gave a linear response up to 15 mM of glucose. A nonlinear current response was observed above this concentration since the rate of glucose diffusion through the PFSA was still high enough that the concentration of oxygen limits the enzymatic reaction rate producing H_2O_2 . A thick 7 μm coating of PFSA significantly reduced the amperometric current, however it also improved the sensor function where a linear sensor response up to 32 mM glucose (slope of current density vs. glucose concentration $\sim 4.8 \times 10^{-3} \mu\text{A} \cdot (\text{mm}^2 \cdot \text{mM})^{-1}$). This linear sensor response is a result of having a membrane thickness that balances the flux of oxygen and glucose through the membrane layer to the enzyme, such that the enzyme reaction is limited by glucose concentration rather than oxygen.

It was previously shown that PFSA could block acetaminophen interference when it is used as an inner membrane.^{35,36} For our glucose sensor PFSA is an outer membrane and it was necessary to determine if this change in structure can also result in blocking interference molecules. The arrows in Figure 6 a indicate when 0.13 mM of acetaminophen, which can oxidize directly on the Pt indicating electrodes,³⁷ was added to the electrolyte at the end of the experiment. A rapid increase in current was observed for the 300 nm PFSA membrane, indicating that acetaminophen readily diffuses through the thin membrane. For the 3 μm thick PFSA membranes there was a slight current increase from the acetaminophen interference. However, interference of acetaminophen was totally suppressed when using a 7 μm thick PFSA membrane, which indicates that thicker PFSA membranes are effective in minimizing interference from acetaminophen.

Conclusions

This study demonstrates that a continuous glucose sensor can be fabricated on flexible polyimide substrate using additive technologies. We were able to use electrohydrodynamic printing to deposit and pattern a biological ink (containing glucose oxidase, bovine serum albumin, and glutaraldehyde as a cross-linking agent) with high resolution on working electrodes. The GOx ink was found to be active even after e-jet printing. PFSA was used as a permselective membrane and its thickness was optimized to obtain a linear response for glucose concentrations up to 32 mM. The flexible sensor design can ultimately be used within a closed loop artificial pancreas control system thereby reducing the number of components in such a system.

Acknowledgements This work was funded by the National Institutes of Health (grant 1-R43-DK-096678-01), Leona M. and Harry B. Helmsley Charitable Trust (grant 2012PG_T1D034), and the Oregon Nanoscience and Microtechnologies Institute (ONAMI). X. Du acknowledges funding support from the Juvenile Diabetes Research Foundation (3-PDF-2014-113-A-N). G. S. Herman thanks John Rogers and Placid Ferreira for providing technical assistance and insight on developing our e-jet printer.

References:

- [1] Block C.D., Manuel-y-Keenoy B., Van Gaal L., *Journal of diabetes science and technology*, **2**, 718 (2008).
- [2] Ward W.K., Castle J.R., Jacobs P.G., Cargill R.S., *Journal of diabetes science and technology*, **8**, 568 (2014).
- [3] Girardin C.M., Huot C., Gonthier M., Delvin E., *Clinical biochemistry*, **42**, 136 (2009).
- [4] Heller A., Feldman B., *Chemical Reviews*, **108**, 2482 (2008).
- [5] Lee H., Buckingham B.A., Wilson D.M., Bequette B.W., *Journal of diabetes science and technology*, **3**, 1082 (2009).
- [6] Mauseth R., Wang Y., Dassau E., Kircher R., Matheson D., Zisser H., et al., *Journal of diabetes science and technology*, **4**, 913 (2010).
- [7] Albisser A.M., Leibel B.S., Ewart T.G., Davidovac Z., Botz C.K., Zingg W., et al., *Diabetes*, **23**, 397 (1974).
- [8] Albisser A.M., Leibel B.S., Ewart T.G., Davidovac Z., Botz C.K., Zingg W., *Diabetes*, **23**, 389 (1974).
- [9] Breton M., Farret A., Bruttomesso D., Anderson S., Magni L., Patek S., et al., *Diabetes*, **61**, 2230 (2012).
- [10] Bruttomesso D., Farret A., Costa S., Marescotti M.C., Vettore M., Avogaro A., et al., *Journal of diabetes science and technology*, **3**, 1014 (2009).
- [11] Kovatchev B., Cobelli C., Renard E., Anderson S., Breton M., Patek S., et al., *Journal of diabetes science and technology*, **4**, 1374 (2010).
- [12] Steil G.M., Rebrin K., Janowski R., Darwin C., Saad M.F., *Diabetes technology & therapeutics*, **5**, 953 (2003).
- [13] Castle J.R., Engle J.M., Youssef J.E., Massoud R.G., Yuen K.C.J., Kagan R., et al., *Diabetes Care*, **33**, 1282 (2010).
- [14] Watson E.M., Chappell M.J., Ducrozet F., Poucher S.M., Yates J.W.T., *Computer Methods and Programs in Biomedicine*, **102**, 119 (2011).
- [15] Weinzimer S.A., Steil G.M., Swan K.L., Dziura J., Kurtz N., Tamborlane W.V., *Diabetes Care*, **31**, 934 (2008).
- [16] Jacobs P.G., El Youssef J., Castle J., Bakhtiani P., Branigan D., Breen M., Bauer D., Preiser N., Leonard G., Stonex T., Ward W.K., *IEEE Trans Biomed Eng.*, **61**, 2569 (2014).
- [17] Castle J.R., Pitts A., Hanavan K., Muhly R., El Youssef J., Hughes-Karvetski C., et al., *Diabetes Care*, **35**, 706 (2012).
- [18] Harrison D.J., Turner R.F.B., Baltes H.P., *Analytical Chemistry*, **60**, 2002 (1988).

- [19] Yu B., Long N., Moussy Y., Moussy F., *Biosensors & bioelectronics*, **21**, 2275 (2006).
- [20] Endo H., Takahashi E., Murata M., Ohnuki H., Ren H., Tsugawa W., et al., *Fisheries Science*, **76**, 687 (2010).
- [21] Kudo H., Sawada T., Kazawa E., Yoshida H., Iwasaki Y., Mitsubayashi K., *Biosensors & bioelectronics*, **22**, 558 (2006).
- [22] Chu M.X., Miyajima K., Takahashi D., Arakawa T., Sano K., Sawada S., et al., *Talanta*, **83**, 960 (2011).
- [23] Li C., Han J., Ahn C.H., *Biosensors & bioelectronics*, **22**, 1988 (2007).
- [24] Love J.C., Estroff L.A., Kriebel J.K., Nuzzo R.G., Whitesides G.M., *Chemical Reviews*, **105**, 1103 (2005).
- [25] Qin D., Xia Y., Whitesides G.M., *Nature protocols*, **5**, 491 (2010).
- [26] Xia Y., Kim E., Zhao X.-M., Rogers J.A., Prentiss M., Whitesides G.M., *Science*, **273**, 347 (1996).
- [27] Geissler M., Wolf H., Stutz R., Delamarche E., Grummt U.-W., Michel B., et al., *Langmuir*, **19**, 6301 (2003).
- [28] Polk B.J., Stelzenmuller A., Mijares G., MacCrehan W., Gaitan M., *Sensors and Actuators B: Chemical*, **114**, 239 (2006).
- [29] Lee M.W., Kang D.K., Kim N.Y., Kim H.Y., James S.C., Yoon S.S., *Journal of Aerosol Science*, **46**, 1 (2012).
- [30] Park J.U., Hardy M., Kang S.J., Barton K., Adair K., Mukhopadhyay D.K., et al., *Nature materials*, **6**, 782 (2007).
- [31] Park J.U., Lee J.H., Paik U., Lu Y., Rogers J.A., *Nano Letters*, **8**, 4210 (2008).
- [32] Wilson D.F., Lee W.M., Makonnen S., Apreleva S., Vinogradov S.A., *Adv Exp Med Biol*. **614**, 53 (2008).
- [33] Moussy F., Harrison D.J., Rajotte R.V., *International Journal of Artificial Organs*, **17**, 88 (1994).
- [34] Valdes T.I., Moussy F., *Biosensors and Bioelectronics*, **14**, 579 (1999).
- [35] Moatti-Sirat D., Poitout V., Thomé V., Gangnerau M.N., Zhang Y., Hu Y., et al., *Diabetologia*, **37**, 610 (1994).
- [36] Vaidya R., Atanasov P., Wilkins E., *Medical engineering & physics*, **17**, 416 (1995).
- [37] Ward W.K., Wood M.D., Troupe J.E., *ASAIO Journal*, **46**, 540 (2000).

Figure 1. (a) On the top, image of the actual device, below schematics of a cross section of the amperometric glucose sensor on polyimide substrate and (b) chemical reactions on Pt working electrodes.

Figure 2. Optical microscopy images of (a) patterned Au on PI substrate prepared via microcontact printing, and (b) Pt and Ag electrodes obtained by electroplating.

Figure 3. E-jet printing of enzyme dots array by 5 μm diameter nozzle at $f = 20$ Hz, $v = 700$ $\mu\text{m/s}$.

Figure 4. Printed GOx with pre-mixed glutaraldehyde on Pt/Au/PI substrate. Optical images of printed dots at (a) $f = 10$ Hz, (b) $f = 20$ Hz, and (c) $f = 30$ Hz, printing speed is constant $v = 1200$ $\mu\text{m/s}$. Optical images of printed patterns at (d) $v = 1200$ $\mu\text{m/s}$, (e) $v = 700$ $\mu\text{m/s}$, and (f) $v = 500$ $\mu\text{m/s}$, pulse frequency is constant $f = 20$ Hz. AFM images (50×50 μm^2) of printed patterns at (g) $v = 1200$ $\mu\text{m/s}$, (h) $v = 700$ $\mu\text{m/s}$, and (i) $v = 500$ $\mu\text{m/s}$, pulse frequency is constant $f = 20$ Hz.

Figure 5. (a) E-jet printing of enzyme ink on Pt working electrodes of glucose sensor and (b) 3D Zscope images of 400×800 μm^2 (working electrode size) pad printed twice over the same area at $f = 20$ Hz, $v = 500$ $\mu\text{m/s}$.

Figure 6. (a) Chronoamperometry of glucose sensor response to glucose concentration with printed GOx on Pt working electrodes and a thin 300 nm, a thick 3 μm and a thick 7 μm outer

PFSA membrane applied in multiple stages. Arrows indicate addition of 0.13 mM acetaminophen. (b) Current density vs. glucose concentration for sensors coated with various PFSA membrane.

Figure 1:

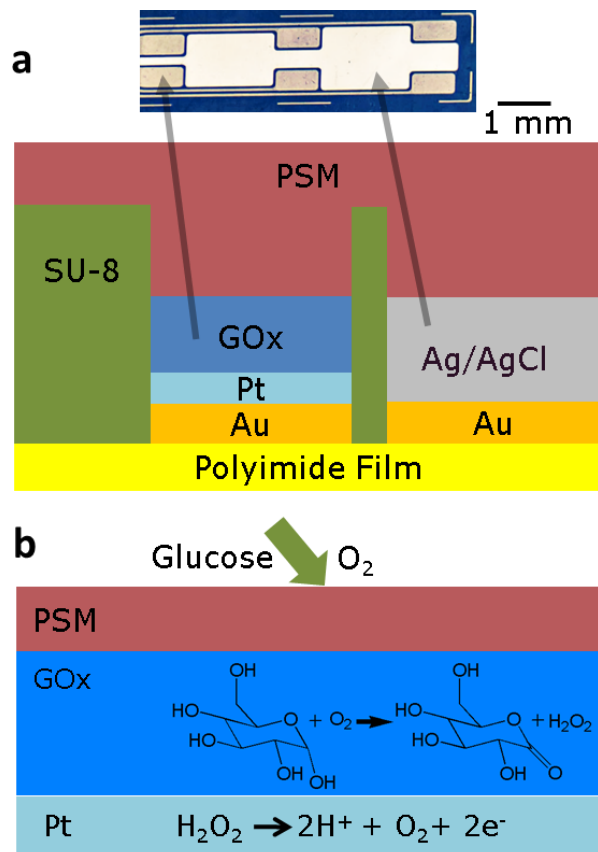


Figure 2:

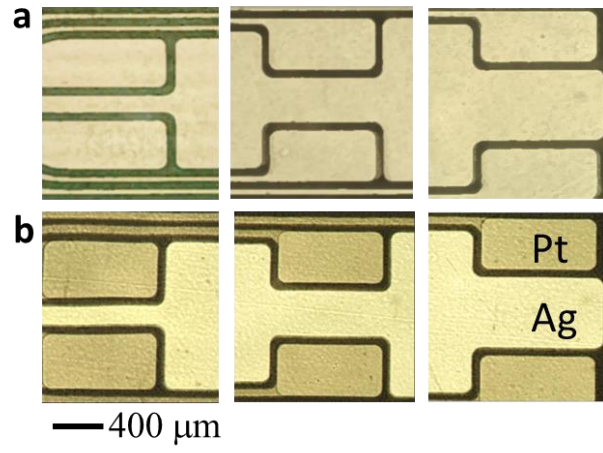


Figure 3:

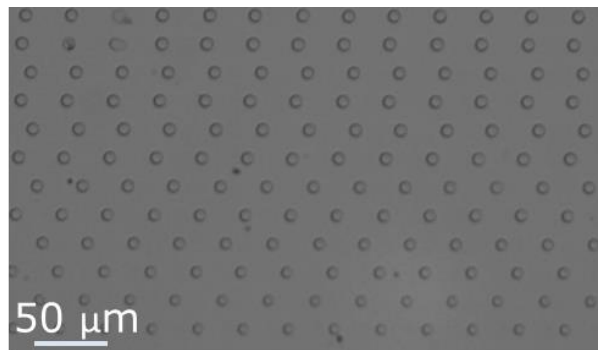


Figure 4:

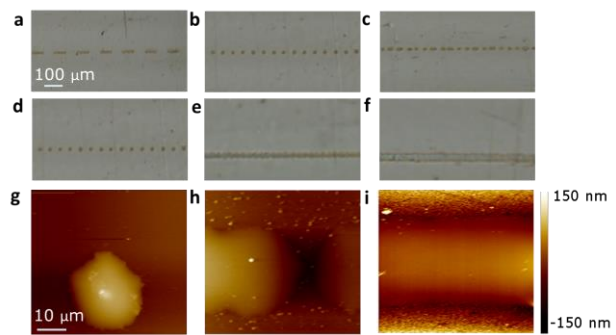


Figure 5:

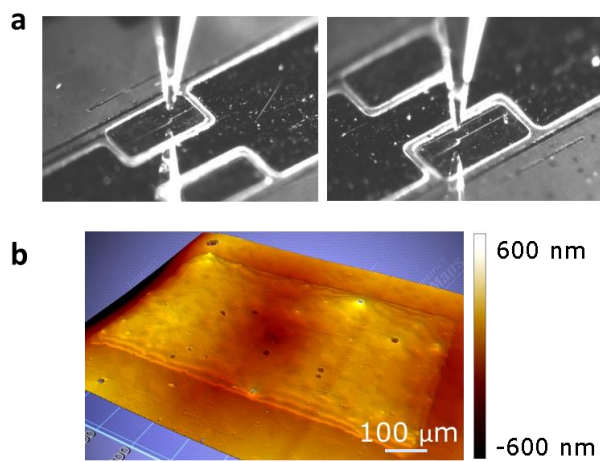


Figure 6:

